NANO LETTERS

2009
Vol. 9, No. 10
3570-3574

Antibiofouling, Sustained Antibiotic Release by Si Nanowire Templates

Karla S. Brammer,[†] Chulmin Choi,[†] Seunghan Oh,[†,‡] Christine J. Cobb,[†] Laura S. Connelly,[†] Mariana Loya,[†] Seong Deok Kong,[†] and Sungho Jin*[,†]

Materials Science & Engineering, University of California, San Diego, La Jolla, California 92093, and Department of Dental Biomaterials, College of Dentistry, Wonkwang University, Iksan, Jeollabookdo, South Korea

Received June 3, 2009

ABSTRACT

Loading or filling nanostructures with antibiotics can be one of the relevant approaches for obtaining a controlled drug release rate. Vertically aligned silicon nanowire (SiNW) arrays with 10−40 nm diameter wires having 1−3 μm in length obtained by the electroless etching (EE) technique are used in this study as novel nanostructures for mediating drug delivery. Here we report controlled antibiotic activity and sustained bioavailability from SiNW arrays and also show microstructural manipulations for a tunable release rate. As well, we have demonstrated biodegradability of SiNWs in phosphate buffer saline (PBS) solution. Strikingly suppressed cell and protein adhesion was observed on our SiNW surface, which indicates a reduced probability for biofouling and drug release impediments. Such antibiotic release from the nanowire-structured surface can provide more reliable antibiotic protection at a targeted implantation or biosensor site.

Introduction. The lack of proper control over a drug release rate and target delivery area is a huge disadvantage for conventional drug tablets. Tablets tend to provide rapid and immediate release of therapeutic agents and require more frequent and repeated dosages for maintaining therapeutic levels, causing unwanted fluctuations in drug amounts delivered to the blood and tissue.[1] In order to circumvent problems in drug adsorption, metabolism, and irregular concentrations and to optimize the therapy itself, a controlled release dosage is advantageous over conventional tablets.[2] Biomaterials with nanoscale features have become increasingly popular as controlled release reservoirs for drug delivery. Nanoscale drug delivery systems can be devised to tune release kinetics, regulate biodistribution, adjust bioavailability over time, and minimize toxic side effects, thus enhancing the therapeutic index of a given drug.[3]

Localization, controlled release, and sustainability of drugs over long periods of time within the body are key challenges in the design of effective drug therapies. Various nanostructured material systems have been developed to meet these challenges. Porous Si templates in particular hold several ideal properties that have been found to be remarkably beneficial.[4−9] Biocompatible porous Si is an attractive material for controlled drug delivery applications for many reasons including the versatility and capability of tailoring the pore sizes (from micrometers to nanometers) and volume of the reservoir, there are numerous existing and convenient chemistries for surface modifications and surface reactions, it can be used as a template for designing polymeric nanostructures, and it has unique optical properties and exceptional biosensing potential.[4]

Here we report a drug release behavior from a quite different nanostructured porous Si template, namely, Si nanowire (SiNW) arrays with a high porosity and surface reactivity and a relatively large reservoir volume. These structural features have spurred our interest in the use of this system as a host or "mothership" for the controlled release of drugs. The electroless etching (EE) approach is used to obtain oriented single crystalline SiNW arrays on silicon substrates which has proven a simple and efficient method to prepare large area samples[10−12] that we have utilized in this study as an antibiotic type drug carrier.

This in vitro experiment was undertaken to determine the release profile of common antibiotics, penicillin/streptomycin (P/S), from SiNW arrays. While sustained drug release from SiNW was the primary aim of this study, we have also observed biodegradability of SiNWs as well as antibiofouling characteristics of such SiNWs with strikingly suppressed cell and protein adhesion on SiNW surface, which indicates a reduced probability for biofouling and drug release impediments.

Materials and Methods. ***Silicon Nanowire (SiNW) Array Fabrication.*** SiNW arrays were prepared using the electroless chemical etching method.[10−12] Briefly, the samples were immersed in a solution composed of 4.6 M HF/0.02 M

* Corresponding author: telephone, 858-534-4903; fax, 858-534-5698; e-mail, jin@ucsd.edu.
[†] University of California, San Diego.
[‡] Wonkwang University.

10.1021/nl901769m CCC: $40.75
Published on Web 07/28/2009

$AgNO_3$ for 20 min. The etching procedure was performed at 50 °C. After the etching process, the samples were immersed in H_2SO_4/H_2O (1:1) to remove the silver dendrites formed during the etching process. The samples were washed several times with distilled water and ethanol. During these steps, the samples were kept in the solution. The regular drying process for the wet etched SiNW samples was performed using nitrogen gas environment. The morphology of the two SiNW arrays was visualized using a FEI field emission scanning electron microscopy (SEM). For the purposes of this study, a bare silicon wafer surface was used as a control surface for all drug and cell assays. All samples were cut into identical size pieces (0.5 × 0.5 in.^{2}) and autoclaved before use.

Drug Loading, Release, and Collection. Insertion of liquid into nanostructures is not always easy as the surface tension of the liquid has to be overcome. At room temperature (25 °C), the SiNW samples were placed in a vacuum ($\sim 10^{-4}$ Torr) for approximately 5−10 min to rid nanopores (between Si nanowires) of any trapped air. Remaining under vacuum, by opening of a control chamber valve, an antibiotic solution was loaded into the samples. The high concentration antibiotic solution loaded was 1 mL of combination antibiotics consisting of 100000 units/mL penicillin + 100000 μg/mL streptomycin (P/S) (from Invitrogen), which is primarily used to prevent bacteria in animal cell cultures. The samples were incubated overnight under vacuum to allow sufficient time for the drug to fully penetrate into the SiNW pore structure. The drug-loaded SiNW samples were washed three times with ice cold (to restrict diffusion from the reservoir) phosphate-buffered saline (PBS), pH 7.4 (Invitrogen). Next, the samples were individually placed in new wells (Nunc, 12-wells) incubated in a humidified 95% air/5% v/v CO_2 incubator at 37 °C in 1 mL of fresh simulated body fluid (PBS was used in this study) for 1 day. The solution was collected at daily time points (days 1−7) and weekly time points thereafter (up to day 42 or 6 weeks) and 1 mL of fresh PBS was added. Drug concentration was determined by measuring the collected solution with a commercial BCA Protein Assay Kit (Pierce) and ThermoMax microplate reader (Molecular Devices, Sunnyvale, CA U.S.A.). Briefly, 25 μL of sample or standard replicate was pipetted into a 96 well microplate (Nunc), 200 μL of BCA working reagent was added to each well, the contents of the plate were mixed on a plate shaker for 30 s and incubated at 37 °C for 30 min, and the solution was read at 560 nm using the ThermoMax microplate reader. The assay was calibrated by use of reagent blanks and standards containing 20−2000 μg of total antibiotics (P/S solution (Invitrogen)). Each sample was read in triplicate. Four samples for each time point were measured and the average values ± standard deviation were graphed to obtain release profiles.

Cell Culture. For this study, MC3T3-E1 mouse osteoblasts (CRL-2593, subclone 4, ATCC, USA) were used. Each 1 mL of cells was mixed with 10 mL of alpha minimum essential medium (α-MEM; Invitrogen, USA) in the presence of 10% fetal bovine serum (FBS; Invitrogen, USA) and 1% penicillin−streptomycin (PS; Invitrogen, USA). The cell suspension was plated in a cell culture dish and incubated under 37 °C, 5% CO_2 environment. When the concentration of the MC3T3-E1 osteoblastic cells reached $\sim 3 \times 10^5$ cells/mL, they were seeded onto the experimental substrates of interest (SiNW or Si Control) which were placed on a 12-well polystyrene plate and stored in a CO_2 incubator for 2 and 24 h to observe cell morphology and count the adhered cells as a function of incubation time using SEM visualization. The concentration of the cells seeded onto the specimen substrate was 5×10^4 cells/well in 1 mL of media.

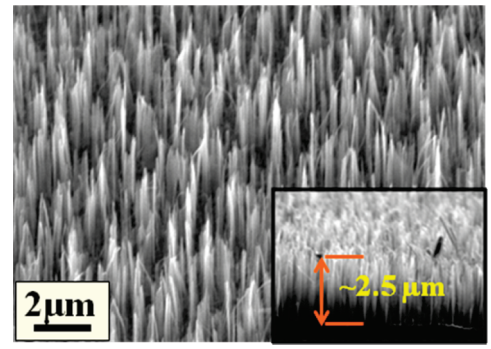

Figure 1. SEM micrograph depicting the vertically aligned Si nanowire (SiNW) morphology (45° tilt) with cross section shown in the inset.

Scanning Electron Microscopy (SEM) for Cell Adhesion and Spreading Analysis. After 2 and 24 h of culture, the cells on the substrates were washed with PBS and fixed with 2.5% (w/v) glutaraldehyde (Sigma, USA) in PBS for 1 h. After fixation, they were washed three times with PBS for 10 min each wash. Then the cells were dehydrated in a graded series of ethanol (50, 70, 90, and 100%) for 30 min each and left in 100% ethanol until they were dried by a critical point dryer (EMS 850, Electron Microscopy Science Co., USA). Next, the dried samples were surface metalized by sputter-coating with gold for SEM (scanning electron microscopy) examination. The morphology of the samples as well as that of the adhered cells was observed using SEM (XL30, FEI Co., USA). In order to quantify the amount of adhered cells and spreading area on experimental specimen SEM images at 2 and 24 h after plating, the cells were analyzed in Image J software, a public domain image processing and analysis program developed by the NIH.

Results and Discussion. The SiNWs are generally aligned vertically parallel to one another as shown in Figure 1. Although many studies have been conducted based on porous Si and drug delivery, this is the first study with this novel nanowire structure. The etched pores are present and the interconnectivity between the nanowire bundles allows for increased surface area and drug loading capacity. This unique nanostructure has increased relative porosity with a more readily reactive surface due to the etching process. It is known that reactive hydride species are left on the surface after fabrication which are available for various reactions and determines the dissolution rate in aqueous media.[4] In this drug delivery system, the antibiotics most likely adsorb and chemically bond to the surface. Especially, it has been observed that sulfate SO_4^{2-} ions, streptomycin sulfate for

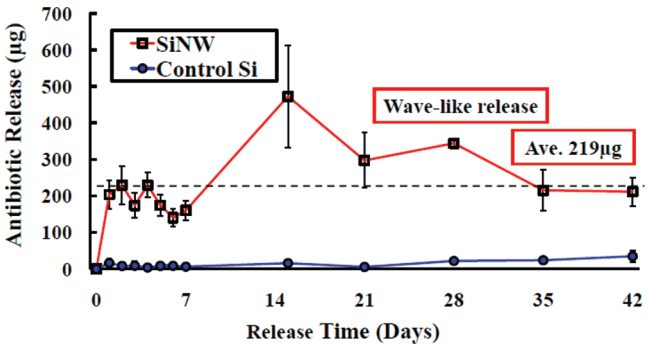

Figure 2. Absolute release of antibiotic measured as a function of sampling time. Mean ± standard deviation is given ($n = 4$). A near constant release is shown over 42 days (6 weeks) and the average amount of antibiotics released for all time points was approximately 219 μg indicated by the dotted line.

instance used in this study, chemically adsorb onto the surface of Si through hydrogen bonds.[4] One advantage to this system (and porous Si in general) is that this type of surface nanostructure has potential to concentrate the drug into the pores for increased loading capability. We have measured the contact angle of water droplet on SiNW and found that the SiNW surface is superhydrophilic, with the contact angle being essentially 0° (the measurement of contact angle was carried out by a video contact angle measurement system, model no. VSA 2500 XE (by AST Products, Inc.). When a water droplet is added to the SiNW surface, it is completely instantaneously absorbed between the nanowire pores. This surface allows for complete and sufficient wetting of the penicillin−streptomycin (P/S) solution for possibly easier and enhanced drug loading capabilities as well.

An antibiotic release profile from the SiNW filled with the (P/S) solution was obtained over 42 days, illustrated in Figure 2. Bare Si wafer controls, without a nanostructured surface topography, showed almost zero antibiotic release as expected. This proved that it was the nanostructure reservoir and surface properties of the SiNW templates that were responsible for the sustained drug release. Note the wavelike aspect of the release in Figure 2 which describes the total amount of antibiotic measured per time point. This shape of release profile is similar to another study using the antibiotic gentamicin (also in the aminoglycoside antibiotic family as streptomycin) release from porous implant materials.[13] Nonetheless, a near steady drug administration is achieved over 42 days with an average release rate over all the time points was ~219 μg. The ideal release profile for most drugs would follow this type of a steady release rate so that the drug levels in the body remain constant while the drug is being administered.[14]

Figure 3a illustrates the accumulative release curve measuring up to 3 mg of antibiotic over 42 days showing near zero-order kinetics over time. The drug is most likely being released as the supporting porous Si matrix is being slowly degraded. Not only is Si biocompatible, but in a biological context it is also bioresorbable. In a recent article it was pointed out that the low toxicity, degradation properties, and solubility of the degradation byproducts of porous Si all combined have generated much interest in its use in controlled drug delivery systems.[4] After 42 days in simulated body fluid (SBF) the substrate has clearly eroded as shown in Figure 3b. The dense SiNW structure of Figure 1 has been substantially deteriorated. The reactions of a variety of porous Si structures with SBF have been monitored similarly using SEM showing significant dissolution.[15,16] This dissolution is mostly due to the high porosity and reactive surface of the nanostructure which can be tailored for a range of biodegradability. For some biomedical applications, especially drug delivery, this type of material corrosion is desirable. Controlled release based on an eroding matrix of SiNWs allows diffusion of the drug from a degrading system with the carrier system itself being not necessarily inert. In our SiNW design and as it has been suggested by others, an active carrier system can sometimes be a part of an additional treatment in terms of contribution to the healing of the surrounding environment tissue.[17] Another attractive advantage to Si degrading in an aqueous solution is that problems related to the removal of the material down the road after use can potentially be avoided.[1]

Sequential and targeted drug delivery could be beneficial when managing a variety of drugs, such as anti-inflammatory agents, antibiotics, chemotherapeutic drugs, steroids, hormones, and vaccines.[17,18] Penicillin and streptomycin, common pharmaceutical antibiotics that reduce the formation of bacteria and biofilms and fights infection, were used as a model drug for our system. With this more advanced drug delivery system, improvements in delivery efficiency and localization may also provide a solution for reducing dosages.[19] Typically, antibiotics are given in large doses up to 1 g/day. But, controlled release, from an implant for instance, would help minimize toxic side effects, drug waste, and further compliance problems that might occur due to prolonged oral antibiotic therapy.[20,21] As well, the steady release rate from SiNW arrays could provide the right amount of drug to continuously meet the "therapeutic window" between the typical systematic drug extremes of overdosages with adverse effects and large amounts of wasted drug and underdosages or being subtherapeutic.

Factors, such as adsorption properties (interactions between drug and matrix), pore size, pore connectivity, pore geometry, and matrix reactions with surrounding media (dissolution properties) are just a few of the aspects to take into account when designing a controlled drug delivery system. We have also explored the option of tailoring the SiNW arrays for changing the drug profiles over time. By increase of the as-fabricated diameters of the nanowires near the top region by sputter coating with an additional ~100−200 nm dimension Si film added on the SiNW tips, an altered nanowire geometry was obtained which enabled us to alter the release rate. A 45° tilted, oblique-incident rf sputtering was carried out under a typical base pressure with the substrate continuously rotated (at a speed of 65 rpm) for improved thickness uniformity. The difference in the nanostructure reservoir geometry with increased bottle-necking SiNW diameters near the nanowire top slowed down the drug release rate by ~25% (data not shown). Additional Si sputter deposition near the

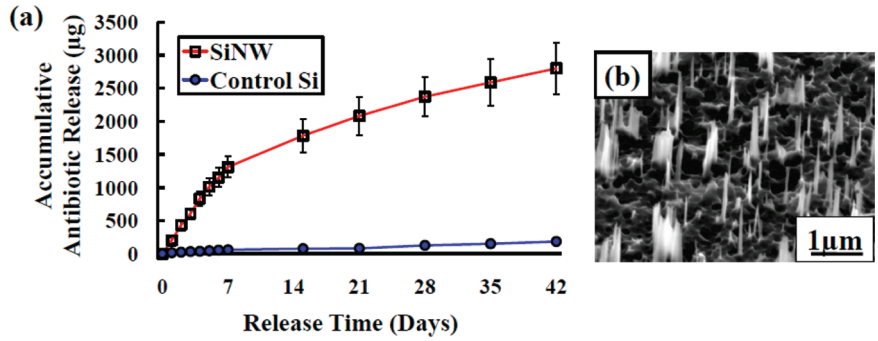

Figure 3. (a) Accumulative release amounts of antibiotics as a function of time showing prolonged release and increased bioavailability from SiNW arrays which are still releasing antibiotics up to day 42. Mean values ± standard deviation bars are given ($n = 4$). (b) SEM micrograph from a portion of the sample surface depicting the SiNW erosion after 42 days in simulated body fluid.

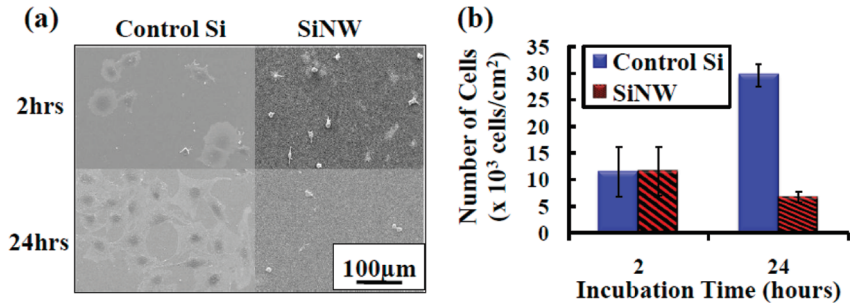

Figure 4. Cell adhesion assay. (a) SEM micrographs showing cell (lighter in color) adhesion on control Si and SiNW surfaces after 2 and 24 h of incubation. The cells on the SiNW surface are unable to spread and adhere compared to cells on the control Si. (b) Quantitative graph depicting the number of adhered cells vs incubation time. The cell number decreases with time on the SiNW surface.

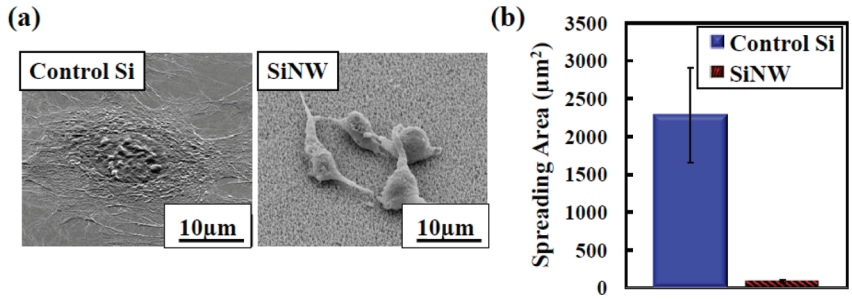

Figure 5. Cell spreading assay. (a) High-magnification SEM micrographs showing cell spreading on control Si and SiNW surfaces after 24 h of incubation. The cells on the SiNW surface are unable to spread and seemingly adhere to each other rather than the surface. (b) Quantitative graph depicting the spreading area of cells using Image J software on the Si vs SiNW surfaces. Cells simply do not spread on SiNW surfaces.

nanowire tip can further reduce the release rate to the extent of ultimately completely blocking the top entrance for a near-zero release rate. In this fashion we were able to control the morphology, dimension, and interface of the SiNW arrays by adding a Si coating and tailoring the release kinetics. The Si coating introduces a necking geometry and possibly surface capping of a portion of the reactive bonds from the electroless etching (EE) process, slowing the dissolution process while the overall reservoir volume was decreased only slightly because of preferential deposition of Si near the nanowire tip.

In terms of biotoxicity, it has been established that there is a relatively low toxicity of porous Si in various cellular and live animal systems.[22−25] However, one of the desired-properties of a drug delivery system is the ability to generate a fully controlled release profile free of cellular adhesion, surface macrophages, or foreign body reactions that would eventually lead to biofouling, impedance, blocking of the pores, and dysfunction of the drug delivery system in general.[26−28] In order to test the cellular attachment to the SiNW surface, we did an initial cell adhesion assay, displayed in Figure 4. We have found a very exciting phenomenon that the SiNWs have the ability to prevent cell adhesion and spreading. As shown in the comparative SEM micrographs of cell adhesion, Figure 4a, it is quite obvious that the cells cannot attach or spread on the SiNW arrays. The cells on the SiNW arrays appear balled up and do not begin spreading. In fact, the number of adhered cells decreases in the first 24 h of incubation because the cells simply cannot adhere to the surface. This could most probably be due to the extremely high surface energy of the SiNW surface. As mentioned previously, the surface contact angle is 0°

indicating superhydrophilicity. This is in agreement with earlier research showing that cells do not adhere or spread on high energy, superhydrophilic surfaces.[29,30] In addition, the nanowire tip contact surface area of approximately 20−40 nm diameter circle, and assuming that approximately half of the Si nanowires are too short to touch the cell because of the extremely uneven surface, it is reasonable that the cells have a hard time attaching to the overall, very small area of available surface. In fact, the spreading of the cells is dramatically reduced on SiNW surfaces compared to control Si as shown in Figure 5. High-magnification SEM images reveal that the cells cannot stick to the surface but instead tend to ball up and are sticking to each other, typically meaning that they do not "like" the surface environment. The overall cell spreading area on the SiNW surface was measured and found to be reduced by a significant factor of ∼25 compared to the flat control Si surface. Another interesting observation to be noted is the low amount of protein adsorption that was observed on the SiNW surfaces when compared to Si controls. When bovine serum albumin (BSA) was incubated with the samples, there was a reduction of protein adhesion by approximately ∼25% (data not shown). This may also have some implications for the increased difficulty of cells adhesion as insufficient protein/integrin contact would reduce cell adhesion. This lack of protein and cell adhesion in the initial in vitro incubation indicates the reduced probability for biofouling and dysfunction due to foreign body reaction cells and proteins in vivo, which has significantly positive implications in the use of SiNWs for a more reliable, nonbiofouling drug delivery system.

In summary, we have shown that SiNW carriers can maintain a drug release level and longevity for 42 days and also report on interesting behavior of the SiNWs preventing cell/protein adhesion. This type of nanowire-based drug release technology may have potential to make significant clinical and industrial impacts. Several interesting therapeutic implications based on our SiNW array drug release are envisioned: (i) a sustained and tailored drug delivery profile for a desired duration of treatment, (ii) a favorable template for appropriate biodegradation, and (iii) an initial antibiofouling interface preventing or minimizing undesirable cell/protein adhesion for various implants, drug delivery vehicles, or biosensors/bioactuators. The SiNW-type controlled release approaches may also be useful for other slow release devices of other drugs, chemicals, pesticides, fertilizers, and/or fragrances.[31]

Acknowledgment. This work was supported by K. Iwama Endowed Chair fund at UC San Diego and UC Discovery biotech research support (Grant No. ele08-128656).

References

(1) Andersson, J.; Rosenholm, J.; Linden, M. Mesoporous Silica: An Alternative Diffusion Controlled Drug Delivery System. In *Topics in Multifunctional Biomaterials and Devices*; Ashammakhi, N., Ed.;E-book, 2008.
(2) Singh, A. The Use of Controlled Release Technology in Drug Delivery. *MURJ* **2000**, *2*, 56.
(3) Kayser, O.; Lemke, A.; Hernandez-Trejo, N. The impact of nanobiotechnology on the development of new drug delivery systems. *Curr. Pharm. Biotechnol.* **2005**, *6* (1), 3–5.
(4) Anglin, E. J.; et al. Porous silicon in drug delivery devices and materials. *Adv. Drug Delivery Rev.* **2008**, *60* (11), 1266–1277.
(5) Begu, S.; et al. Preparation and characterization of siliceous material using liposomes as template. *Chem. Commun. (Cambridge, U.K.)* **2003**, (5), 640–641.
(6) Charnay, C.; et al. Inclusion of ibuprofen in mesoporous templated silica: drug loading and release property. *Eur. J. Pharm. Biopharm.* **2004**, *57* (3), 533–540.
(7) Li, Y. Y.; et al. Polymer replicas of photonic porous silicon for sensing and drug delivery applications. *Science* **2003**, *299* (5615), 2045–2047.
(8) Tourne-Peteilh, C.; et al. The potential of ordered mesoporous silica for the storage of drugs: the example of a pentapeptide encapsulated in a MSU-tween 80. *ChemPhysChem* **2003**, *4* (3), 281–286.
(9) Wu, E. C.; Park, J.-H.; Park, J.; Segal, E.; Cunin, F.; Sailor, M. J. Oxidation-triggered release of fluorescent molecules or drugs from mesoporous Si microparticles. *ACS Nano* **2008**, *2* (11), 2401–2409.
(10) Peng, K. Q.; et al. Synthesis of large-area silicon nanowire arrays via self-assembling nanoelectrochemistry. *Adv. Mater.* **2002**, *14* (16), 1164–1167.
(11) Peng, K. Q.; et al. Uniform, axial-orientation alignment of one-dimensional single-crystal silicon nanostructure arrays. *Angew. Chem., Int. Ed.* **2005**, *44* (18), 2737–2742.
(12) Fang, H.; et al. Silver catalysis in the fabrication of silicon nanowire arrays. *Nanotechnology* **2006**, *17* (15), 3768–3774.
(13) Teller, M.; et al. Release of gentamicin from bone regenerative materials: an in vitro study. *J. Biomed. Mater. Res., Part B* **2007**, *81* (1), 23–29.
(14) Hughes, G. A. Nanostructure-mediated drug delivery. *DM Dis.-Mon.* **2005**, *51* (6), 342–361.
(15) Canham, L. T. Bioactive silicon structure fabrication through nanoetching techniques. *Adv. Mater.* **1995**, *7* (12), 1033.
(16) Canham, L. T. Derivatized mesoporous silicon with dramatically improved stability in simulated human blood plasma. *Adv. Mater.* **1999**, *11* (18), 1505.
(17) Kim, C.-J. *Controlled release dosage form design*; Technomic Publishing Company, Inc.: Lancaster, PA, 2000.
(18) Uhrich, K. E.; et al. Polymeric systems for controlled drug release. *Chem. Rev.* **1999**, *99* (11), 3181–3198.
(19) LaVan, D. A.; McGuire, T.; Langer, R. Small-scale systems for in vivo drug delivery. *Nat. Biotechnol.* **2003**, *21* (10), 1184–1191.
(20) Ramchandani, M.; Robinson, D. In vitro and in vivo release of ciprofloxacin from PLGA 50:50 implants. *J. Controlled Release* **1998**, *54* (2), 167–175.
(21) van de Belt, H.; et al. Infection of orthopedic implants and the use of antibiotic-loaded bone cements. A review. *Acta Orthop. Scand.* **2001**, *72* (6), 557–71.
(22) Bayliss, S. C.; et al. The culture of neurons on silicon. *Sens. Actuators, A* **1999**, *74* (1−3), 139–142.
(23) Sapelkin, A. V.; et al. Interaction of B50 rat hippocampal cells with stain-etched porous silicon. *Biomaterials* **2006**, *27* (6), 842–846.
(24) Low, S. P.; et al. The biocompatibility of porous silicon in tissues of the eye. *Biomaterials* **2009**, *30* (15), 2873–2880.
(25) Low, S. P.; et al. Evaluation of mammalian cell adhesion on surface-modified porous silicon. *Biomaterials* **2006**, *27* (26), 4538–4546.
(26) Santini, J. T., Jr.; Cima, M. J.; Langer, R. A controlled-release microchip. *Nature* **1999**, *397* (6717), 335–338.
(27) Voskerician, G.; et al. Biocompatibility and biofouling of MEMS drug delivery devices. *Biomaterials* **2003**, *24* (11), 1959–1967.
(28) Santini, J. T., Jr. Microchip technology in drug delivery. *Ann. Med. (Basingstoke, U.K.)* **2000**, *32* (6), 377–379.
(29) Horbett, T. A.; Schway, M. B. Correlations between mouse 3T3 cell spreading and serum fibronectin adsorption on glass and hydroxyethylmethacrylate-ethylmethacrylate copolymers. *J. Biomed. Mater. Res.* **1988**, *22* (9), 763–793.
(30) van Wachem, P. B.; et al. Interaction of cultured human endothelial cells with polymeric surfaces of different wettabilities. *Biomaterials* **1985**, *6* (6), 403–408.
(31) Langer, R. New methods of drug delivery. *Science* **1990**, *249* (4976), 1527–1533.

NL901769M